ASTRONOMY
AND
ASTROPHYSICS

Near-infrared imaging of the host galaxies
of flat spectrum radio quasars[*]

Jari K. Kotilainen[1,2], **Renato Falomo**[3], **and Riccardo Scarpa**[4]

[1] International School for Advanced Studies (SISSA), via Beirut 2-4, I-34014 Trieste, Italy (jkotilai@sissa.it)
[2] Tuorla Observatory, University of Turku, Väisäläntie 20, FIN-21500 Piikkiö, Finland
[3] Osservatorio Astronomico di Padova, vicolo dell'Osservatorio 5, I-35122 Padova, Italy (falomo@astrpd.pd.astro.it)
[4] Space Telescope Science Institute, 3700 San Martin Drive, Baltimore, MD 21218, USA (scarpa@stsci.edu)

Abstract. We present the results of a high resolution ($0.27''$ px^{-1}) near-infrared H band (1.65 μm) imaging survey of a complete sample of 20 flat spectrum radio quasars (FSRQ) extracted from the 2Jy catalogue of radio sources (Wall & Peacock 1985). The observed objects are intrinsically luminous with median M(B) = -25.5. The median redshift of the objects in the sample is z = 0.65. At this redshift, the H band observations probe the old stellar population of the hosts at rest frame wavelength of $\sim$1 μm.

We are able to detect the host galaxy clearly for six (30 %) FSRQs and marginally for six (30 %) other FSRQs, while the object remains unresolved for eight (40 %) cases. We find the galaxies hosting FSRQs to be very luminous (M(H)$\sim$-27). Compared with the typical galaxy luminosity L* (M*(H)$\sim$-25) they appear $\sim$2 mag brighter, although the undetected hosts may reduce this difference. They are also at least as bright as, and probably by $\sim$1 mag brighter than, the brightest cluster galaxies (M(H)$\sim$-26). The luminosities of the FSRQ hosts are intermediate between host galaxies of low redshift radio-loud quasars and BL Lac objects (M(H)$\sim$-26), and the hosts of high redshift radio-loud quasars (M(H)$\sim$-29), in good agreement with current unified models for radio-loud AGN, taking into account stellar evolution in the elliptical host galaxies. Finally, we find an indicative trend between the host and nuclear luminosity for the most luminous FSRQs, supporting the suggestion based on studies of lower redshift AGN, that there is a minimum host galaxy luminosity which increases linearly with the quasar luminosity.

Key words: BL Lac objects: general – galaxies: active – galaxies: nuclei – infrared: galaxies – quasars: general

---

1. Introduction

The determination of the properties of the host galaxies of different types of active galactic nuclei (AGN) is a key tool for our understanding of the AGN phenomenon and for unification of different types of AGN. Comparison of AGN properties not affected by orientation effects (e.g. host galaxies) provides a crucial test of the current unified models (Antonucci 1993; Urry & Padovani 1995). Also, it sheds light on the role played by the environment for triggering of nuclear activity (Hutchings & Neff 1992) and on the effect of the AGN on its host.

Flat spectrum radio quasars (FSRQ) form a distinct group from "normal" steep spectrum radio-loud quasars (RLQ). Most quasars with radio spectral index $\alpha_R >$-0.5 (f$_\nu \propto \nu^{+\alpha}$) are characterized by rapid variability, high and variable polarization and high brightness temperatures (Fugmann 1988; Impey & Tapia 1990; Quirrenbach et al. 1992). Moreover, almost all FSRQs in complete samples (Wall & Peacock 1985) are core-dominated radio sources and objects observed at different epochs with VLBI display superluminal motion (Padovani & Urry 1992; Vermeulen & Cohen 1994). FSRQs share many observed properties with BL Lac objects and they are often grouped together into a common class of blazars. The main difference between the two classes is that while FSRQs have strong broad emission lines of similar intensity to "normal" quasars, emission lines are very weak or absent in BL Lacs. How much of the distinction between BL Lacs and FSRQs is due to intrinsic properties or a consequence of the classification criteria remains unclear, indeed by definition BL Lacs are required to have emission line equivalent width smaller than 5 Å, otherwise they are classified as FSRQs. This selection bias may be responsible for the reported emission line differences (Scarpa & Falomo 1997). On the other hand, based on their extended radio emission and evolutionary properties (Stickel et al. 1991; Padovani 1992) the two groups of blazars appear different.

The rapid variability, high polarization and high luminosity of blazars are usually explained in terms of synchrotron radi-

ation strongly relativistically beamed close to our line-of-sight (Blandford & Rees 1978). This is supported by the fact that practically all blazars are luminous and rapidly variable γ-ray sources (e.g. von Montigny et al. 1995). If the beaming hypothesis is correct, it implies the existence of a more numerous parent population of objects intrinsically identical to blazars, but with the jet directed away from our line of sight. In the unified schemes (Barthel 1989; Urry & Padovani 1995), that interpret different classes of objects based on geometry, the currently favoured model identifies the parent objects of FSRQs with high luminosity lobe-dominated (F-R II) radio galaxies (RG), while the low luminosity core-dominated (F-R I) RGs represent the parents of BL Lacs (Browne 1983; Ulrich 1989; Padovani & Urry 1992). A comparison of statistical properties of FSRQ and BL Lac samples (Padovani 1992) suggests that the two classes of blazars represent similar activity phenomena occurring in high- and low-luminosity early type galaxies, respectively. However, there exist potential problems in this simple unification, such as the discrepant linear radio sizes of RGs and RLQs, dependence on redshift of the ratio of RLQs to RGs, the lack of superluminal motion in RGs, and the discrepant radio morphologies of some BL Lacs with respect to F-R I RGs (see Urry & Padovani 1995).

While some effort has gone to study the properties of BL Lacs (e.g. Falomo 1996; Wurtz, Stocke & Yee 1996; and references therein), no systematic investigation of the host properties of FSRQs has so far been undertaken. In this paper we present the first deep high spatial resolution ($0.27''$ px^{-1}, $\sim 1''$ FWHM) near-infrared (NIR) imaging study of the host galaxies of a complete sample of FSRQs in the H (1.65 μm) band. While most work on AGN host galaxies has traditionally been done in the optical, the NIR wavelengths offer many advantages. Optical emission from quasars is strongly dominated by the nuclear source. Often the host galaxies are interacting systems and appear irregular in the optical because of tidal distortion, star formation and dust emission. The luminosity of the massive old stellar population, on the other hand, peaks in the NIR, leading to a minimum nucleus/host ratio there. With increasing redshift, one also needs to apply much lower K-correction than in the optical.

The FSRQ sample is taken from the 2Jy (Wall & Peacock 1985) catalogue of radio sources, including all flat spectrum sources at z<1.0, at declination δ <20° and not classified as BL Lacs. This yields a total of 20 sources. General properties of the objects are given in Table 1. For information of the radio and X-ray properties of the sample, see Padovani (1992) and Sambruna (1997), respectively. We investigate the properties of the host galaxies of FSRQs using 1-D luminosity profile decomposition into nuclear and galaxy components. We compare the host absolute magnitudes and scale lengths with those of BL Lac hosts, "normal" RLQ hosts and RGs, and study the relationship between host galaxies and nuclear activity.

This paper is arranged as follows. In Sect. 2, we describe the observations and data reduction. Sect. 3 gives the modelling of the profiles, while in Sect. 4 we present the derived host parameters and discuss the properties of the sample with respect to other classes of AGN. Conclusions are given in Sect. 5. In the

Table 1. The sample

Name	Other name	z	V	M(B)
PKS 0208 − 512		1.003	16.9	-26.8
PKS 0336 − 019	CTA 26	0.852	18.4	-24.9
PKS 0403 − 132	OF-105	0.571	17.1	-25.4
PKS 0405 − 123	OF-109	0.574	14.9	-27.7
PKS 0420 − 014	OF-035	0.915	17.0	-26.5
PKS 0440 − 003	NRAO 190	0.844	19.2	-24.3
PKS 0454 − 463		0.858	17.4	-26.5
PKS 0605 − 085	OH-10	0.872	18.5	-25.4
PKS 0637 − 752		0.654	15.7	-27.0
PKS 0736 + 017	OI 61	0.191	16.5	-23.5
PKS 1055 + 018	4C 01.28	0.888	18.3	-25.3
PKS 1226 + 023	3C 273	0.158	12.8	-26.9
PKS 1253 − 055	3C 279	0.538	17.7	-24.6
PKS 1504 − 166	OR-107	0.876	18.5	-25.5
PKS 1510 − 089	OR-017	0.361	16.5	-25.1
PKS 1954 − 388		0.626	17.1	-25.3
PKS 2128 − 123	OX-148	0.501	16.1	-26.1
PKS 2145 + 067	4C 06.69	0.990	16.5	-27.4
PKS 2243 − 123	OY-172.6	0.630	16.4	-26.4
PKS 2345 − 167	OZ-176	0.576	18.4	-24.1

Appendix (http://link.springer.de), we compare our results for individual objects with existing results in the literature. Hubble constant H_0 = 50 km s^{-1} Mpc^{-1} and deceleration parameter q_0 = 0 are used throughout this paper.

2. Observations and data reduction

We have obtained NIR broad-band images at H (1.65 μm) band of 20 FSRQs. The observations were carried out during two observing runs (in August 1995 and January 1996) at the ESO/MPI 2.2m telescope at the European Southern Observatory (ESO), La Silla, Chile. We used the 256×256 px IRAC2 NIR camera (Moorwood et al. 1992) and pixel scale 0.27$''$ px^{-1}, giving a field of view of 69 arcsec^2. Details of the observations and NIR photometry are given in Table 2. We shifted the target in a 2×2 grid across the array between the observations with typical offsets of 30$''$, thus keeping the target always in the field and using the other exposures as sky frames. Individual exposures were of 60 sec duration; these were coadded to achieve the final integration time.

Data reduction was performed using IRAF. First, from a raw flat-field frame, we marked all bad pixels that were subsequently corrected for in all flat-field and science frames by interpolating across neighboring pixels. The corrected ON and OFF flat-field frames were subtracted from each other, and in case of several ON-OFF pairs, averaged together. The resulting flat-fields for each filter and each night were finally normalized to create the final flat-fields. For each science frame, a sky frame was produced by median averaging all the other frames in a grid. This median sky frame was then scaled to match the median intensity level of the science frame, and subtracted. Finally, flat-field

Table 2. Journal of observations.

Name	Date	T_{int} min	FWHM arcsec	$6''$ ap. mag
PKS $0208-512$	19/8/95	6	1.2	11.76
	21/8/95	20	1.1	11.70
PKS $0336-019$	12/1/96	72	1.0	16.39
PKS $0403-132$	11/1/96	60	1.2	14.97
PKS $0405-123$	13/1/96	27	0.8	13.33
PKS $0420-014$	12/1/96	69	0.9	13.62
PKS $0440-003$	13/1/96	75	1.0	16.04
PKS $0454-463$	11/1/96	66	1.0	15.91
PKS $0605-085$	12/1/96	42	0.9	12.71
PKS $0637-752$	12/1/96	72	1.0	14.79
PKS $0736+017$	11/1/96	45	0.9	13.66
PKS $1055+018$	11/1/96	51	0.9	15.19
PKS $1226+023$	12/1/96	20	0.9	10.92
PKS $1253-055$	21/8/95	40	2.0	12.92
PKS $1504-166$	18/8/95	40	1.3	17.40
PKS $1510-089$	20/8/95	40	2.0	13.29
PKS $1954-388$	19/8/95	60	0.9	14.15
PKS $2128-123$	18/8/95	80	0.9	14.32
PKS $2145+067$	21/8/95	60	1.1	14.47
PKS $2243-123$	18/8/95	40	0.9	14.91
PKS $2345-167$	18/8/95	60	0.8	13.43

correction was applied to each sky-subtracted frame to produce the final reduced images. All the images of the same target were then aligned, using field stars or the centroid of the light distribution of the object as a reference point, and combined in order to produce the final reduced images that will be used in the subsequent analysis.

Standard stars from Landolt (1992) were observed frequently throughout the nights to provide the photometric calibration zero points. We estimate photometric accuracy of $\sim\pm0.1$ mag. K-correction was applied to the host galaxy magnitudes following the method of Neugebauer et al. (1985; their Table 3) for a first-ranked elliptical galaxy. The applied K-correction for each source is reported in Table 3, column 3. The size of the correction, insignificant at low redshift, is m(H)$\sim$0.14 at our median redshift of z = 0.65. No K-correction was applied to the nuclear quasar component, since for a power law spectrum the K-correction equals to $(1 + z)^{1+\alpha}$, where $\alpha\sim$ -1 for quasars.

3. Modelling of the luminosity profiles

Because of the relatively high redshift of the quasars, the extended emission around them is faint and consequently rather noisy. Therefore, in our analysis we have considered only the azimuthally averaged fluxes. After masking all the regions around the target contaminated by companions, we have derived for each object the radial luminosity profile out to a radius where the signal was not distinguished from the background noise. This corresponds typically to surface brightness of $\mu(H) = 23$-24 mag arcsec^{-2}, depending on exposure time and observing conditions. Similar procedure was followed for the field stars

(when available), to obtain the point spread function (PSF) suitable for each image. Since the field of view is small, only for few objects a star of brightness comparable (or brighter) to the target was present in the observed field. For most sources only fainter stars were available, therefore extrapolation of the PSF was required at the lowest flux levels. This extrapolation is particularly important for marginally resolved objects for which the reliability of derived host properties strongly depends on the assumed PSF shape.

We have adopted a functional form to describe the shape of the PSF as a Moffat (1969) function, characterized by σ for the core and β for the wings of the PSF. A fit of a Moffat function to the shape of the profiles of the available bright stars was found to be quite a good representation of the observed PSF. In order to describe the shape of the PSF for fields with no stars or only faint stars, we have determined σ from fitting the core of the stellar profile, whereas β was derived from the values obtained by fitting bright stars in other frames observed during the same night with similar seeing conditions. For a few objects, no stars were visible in the observed field and in these cases the target itself, which is always dominated by the nuclear source, was used to estimate σ and β as described above.

The luminosity profiles were fitted into a point source (described by the PSF) and a galaxy (described by de Vaucouleurs law, convolved with the PSF) components by an iterative least-squares fit to the observed profile. Noisy outer parts of the profiles were rejected from the fit. There are three free parameters in our fitting: the PSF and bulge intensities at the center, and the effective radius of the bulge. We also tried to fit a number of profiles with a combination of a PSF and a disk, and although in many cases no significant difference was found with respect to an elliptical fit, in no case did the disk model yield a better fit. This is not surprising, since RLQs are expected to be hosted in early-type galaxies, as well demonstrated for low redshift objects by e.g. Taylor et al. (1996; hereafter T96) and Bahcall et al. (1997). For sources with no host galaxy detected in our observations, we determined an upper limit to the brightness of the host galaxy by adding simulated "host galaxies" of various brightness to the observed profile until the simulated host became detectable within the errors of the luminosity profile.

A main problem with the fitting is related to the uncertainty in the sky background level. We have checked this by adding or subtracting counts, corresponding to 1 σ level of the background around the target, from the observed profiles, and redoing the fits. The derived host parameters do not change much. Another problem is the existence of multiple minima in the χ^2-fit, e.g. several r(e)-μ(e) pairs can fit the data almost equally well. Note that r(e) and μ(e) are expected to be correlated, for the total galactic luminosity to be accurately reproduced (see e.g. T96). We have checked the severity of this problem by starting the fit from various different initial values. In general, the fitting program always finds roughly the same best values, more easily so for sources with a clearly resolved host galaxy. We estimate an error in the derived host galaxy magnitudes to be $\sim\pm0.3$ mag for the clearly detected hosts, this error being largest for the sources with the largest nucleus-to-galaxy luminosity ra-

tio. For the marginally detected hosts, due to the uncertainties mentioned above, we can only assess a lower limit to the error margin as $\geq\pm0.5$.

The fact that we find a very good agreement with previous studies on the derived host luminosity for two low redshift FS-RQs in our sample (PKS 0736+01 and PKS 1226+023 = 3C 273; see Appendix at http://link.springer.de) gives us confidence in our adopted procedure also for the more problematic derivation of host properties in our higher redshift sources. We also note that one of the marginally resolved objects, PKS 2128-123 at z = 0.501, has been clearly resolved in the I-band by the HST (Disney et al. 1995). The host magnitude we derive in the H-band is ~1 mag fainter than expected from the I-band for normal galaxy colours. However, this difference is not unreasonable, taking into account all the uncertainties mentioned above.

4. Results and discussion

In Fig. 1a we show the H band contour plots of all the FSRQs, after smoothing the images with a Gaussian filter of $\sigma = 1$ px. We detect the host galaxy clearly for six (30 %) FSRQs and marginally for six (30 %) more. The host remains unresolved for eight (40 %) FSRQs out of 20. We summarize our results in Table 3, which gives the best-fit model parameters of the profile fitting and the derived properties of the host galaxies. In Fig. 1b (http://link.springer.de), we show the profiles of each FSRQ, with the best-fit models overlaid. Table 4 presents a comparison of the H band absolute magnitudes of the FSRQ hosts with relevant samples from previous studies in the literature, for which we report the average values after correcting the published values for color term and to our cosmology ($H_0 = 50$). In the Appendix (http://link.springer.de), we compare our NIR photometry with previous existing studies, and discuss in more detail individual quasars, including comparison with previous optical/NIR determinations of the host galaxies.

4.1. Host luminosity

In Fig. 2 (upper panel) we investigate the location of the FSRQ hosts and the hosts of various other AGN samples imaged in the NIR in the apparent magnitude vs. redshift H-z Hubble diagram, relative to the established relation for RGs (solid line, e.g. Lilly & Longair 1984; Lilly, Longair & Allington-Smith 1985; Eales et al. 1997). For comparison, we also show the evolutionary model for elliptical galaxies derived from passive models of stellar evolution by Bressan, Chiosi & Fagotto (1994; dashed line, normalized to the average redshift and magnitude of the T96 low redshift RGs). The resolved FSRQ hosts lie remarkably well on the H-z relation, whereas there is large scatter for the marginally resolved FSRQ hosts. In Fig. 2 (lower panel) we show the H-z diagram for the mean value of various samples of AGN taken from the literature. T96 found for nearby RLQ and RG hosts (after removing the nuclear component) that they lie above the established RG relation, i.e. toward fainter magnitude by ~ 0.5 mag on the average. It is apparent that the same holds true for most other low redshift AGN samples and, at interme-

diate redshift, for the marginally resolved FSRQ hosts and for the RLQ hosts of Hooper, Impey & Foltz (1997). This may indicate a continuation, and even strengthening, of the deviation found by T96 to higher redshift which is likely explained by the (uncorrected) contribution of the nuclear source in RGs (see T96).

Interestingly, however, the firmly detected FSRQ hosts (and the intermediate redshift RLQ hosts of Rönnback et al. 1996) have relatively brighter magnitudes than the low redshift RLQs and the intermediate redshift RLQs of Hooper et al. (1997), consistent with the established RG relation (solid line in Fig. 2). Also, the magnitudes of the high redshift (z~2) RLQ hosts studied by Lehnert et al. (1992) are consistent with the H-z relation, suggesting that between redshifts of z~0.5 and z~2 there is an increase in the host brightness with respect to the Hubble diagram. Similar result for high redshift RGs was noted by Eales et al. (1997) who found that while the Hubble diagram of luminous 3C RGs and fainter 6C/B2 RGs were similar at z<0.6, the 3C RGs are ~0.6 mag brighter at z>1. Eales et al. attribute this change not to stellar evolution, but to a difference in the intrinsic luminosity of the AGN component of the RG samples studied. There is also an obvious selection effect in that at very high redshifts, only very bright host galaxies can be detected (see also Fig. 3).

In Fig. 3, we show the H band absolute magnitude vs. redshift for the host galaxies from various samples. The average H band absolute magnitude of the resolved FSRQ host galaxies is M(H) = -27.4$\pm$0.6 and the average bulge scale length 11.6$\pm$7.6 kpc, while the values after adding the marginally resolved hosts are -26.7$\pm$1.2 and 12.8$\pm$6.0 kpc. The absolute magnitude considering only the four resolved FSRQs at 0.5<z<1.0 is M(H) = -27.8$\pm$0.3. The FSRQ hosts are therefore large (all have R(e)>3 kpc, the empirical upper boundary found for normal local ellipticals by Capaccioli, Caon & D'Onofrio 1992), and very luminous, much brighter than the luminosity of an L* galaxy, which has M(H) = -25.0$\pm$0.3 (Mobasher, Sharples & Ellis 1993). It is therefore evident that the clearly detected FSRQ hosts are preferentially selected from the high-luminosity tail of the galaxy luminosity function (the derived upper limits for the unresolved hosts are also consistent with this). Indeed, we find no case of an FSRQ host with M(H)>-25, indicating that for some reason these quasars cannot be hosted by a galaxy with L<L* (similarly to what was found by T96). The FSRQ hosts have also slightly brighter luminosities than the mean value of brightest cluster member galaxies (BCM; M(H) = -26.3$\pm$0.3; Thuan & Puschell 1989), although there are several FSRQ hosts that fall into the BCM range.

Most of the available comparison data are for low and intermediate redshift RLQs. The samples we have retrieved from literature span a moderately large range in redshift from z~0.1 up to z~0.6, slightly smaller than the average redshift of the FSRQ sample. The average host galaxy magnitudes for the various samples are given in Table 4. The RLQ samples we consider are (in order of increasing average redshift) from McLeod & Rieke (1994a,b), Bahcall et al. (1997), T96, Veron-Cetty & Woltjer (1990), Hooper et al. (1997) and Rönnback et al. (1996).

Table 3. Properties of the host galaxies.

Name	z	K-corr.	r(e)/R(e) ($''$/kpc)	m_H nucleus	m_H host	L(n)/L(g)	M_H nucleus	M_H host	Note[*]
PKS 0208 − 512	1.003	0.30	1.85/20.2	11.8	15.0	19.0	-33.2	-30.3	M
PKS 0336 − 019	0.852	0.22		16.2	>16.6	>1.4	-28.2	>-28.0	U
PKS 0403 − 132	0.571	0.12	2.75/23.8	14.9	18.8	32.3	-28.8	-25.1	M
PKS 0405 − 123	0.574	0.12	1.20/10.4	13.4	15.6	8.1	-30.0	-27.9	R
PKS 0420 − 014	0.915	0.25	2.45/25.9	13.5	17.0	24.0	-31.4	-28.1	R
PKS 0440 − 003	0.844	0.21		16.0	>17.5	>4.0	-28.3	>-27.0	U
PKS 0454 − 463	0.858	0.22		15.9	>18.1	>7.6	-28.5	>-26.5	U
PKS 0605 − 085	0.872	0.23							U
PKS 0637 − 752	0.654	0.14	1.35/12.5	14.6	17.8	19.0	-29.2	-26.1	M
PKS 0736 + 017	0.191	0.01	0.75/ 3.2	14.3	14.3	1.0	-26.2	-26.2	R
PKS 1055 + 018	0.888	0.23		15.2	>17.7	>10.0	-29.3	>-27.0	U
PKS 1226 + 023	0.158	0.01	4.50/16.6	10.9	13.3	9.0	-29.4	-27.0	R
PKS 1253 − 055	0.538	0.12		12.9	>13.7	>2.1	-29.6	>-29.0	U
PKS 1504 − 166	0.876	0.23		17.6		> 100	-26.9		U
PKS 1510 − 089	0.361	0.04		14.8	>16.2	>3.6	-27.3	>-26.0	U
PKS 1954 − 388	0.626	0.14	0.65/ 5.9	14.1	16.3	7.3	-29.4	-27.3	R
PKS 2128 − 123	0.501	0.11	2.00/16.0	13.9	18.0	44.0	-29.0	-25.1	M
PKS 2145 + 067	0.990	0.29	1.05/11.4	14.4	17.7	19.0	-30.5	-27.5	M
PKS 2243 − 123	0.630	0.14	0.80/ 7.3	14.8	18.2	24.0	-28.9	-25.5	M
PKS 2345 − 167	0.576	0.13	0.90/ 7.8	13.3	15.7	9.0	-30.1	-27.8	R

[*]: R = resolved, M = marginally resolved, U = unresolved.

Table 4. Comparison of the average host galaxy properties with other samples.

| Sample	filter	N	$< z >$	$< M_B >$	$< M_H(nuc) >$	$< M_H(host) >$[b]
L[*] Mobasher et al. (1993)	K	136	0.077±0.030			-25.0±0.2
BCM Thuan & Puschell (1989)	H	84	0.074±0.026			-26.3±0.3
RLQ McLeod & Rieke (1994a)	H	22	0.103±0.029		-25.1±0.5	-24.9±0.6
RLQ McLeod & Rieke (1994b)	H	23	0.196±0.047		-26.5±0.9	-25.7±0.6
RLQ Bahcall et al. (1997)	V	6	0.220±0.047	-25.5±0.9		-26.1±0.5
RLQ Taylor et al. (1996)	K	13	0.236±0.046	-24.5±0.8	-27.1±0.8	-26.3±0.7
RLQ Veron-Cetty & Woltjer (1990)	I	20	0.343±0.094	-25.2±0.5		-26.3±0.5
RLQ Hooper et al. (1997)	R	6	0.465±0.032		-26.8±0.4	-26.2±0.4
RLQ Rönnback et al. (1996)	R	9	0.594±0.120	-24.7±1.1		-25.8±0.4
RLQ Lehnert et al. (1992)	K	6	2.342±0.319		-30.5±1.0	-28.8±1.1
RG Taylor et al. (1996)	K	12	0.214±0.049	-21.7±0.6	-25.1±0.7	-26.1±0.8
BL Falomo (1996), Wurtz et al. (1996)	R	48	0.194±0.101		-25.2±2.4	-26.3±0.7
BL Falomo et al. (1997)	I	7	0.422±0.186		-27.0±0.8	-26.7±0.8
FSRQ/R+M[a] (0.5<z<1.0)	H	9	0.671±0.157	-26.2±1.1	-29.7±0.8	-26.7±1.2
FSRQ/R[a] (0.5<z<1.0)	H	4	0.673±0.141	-25.9±1.3	-30.2±0.7	-27.8±0.3

[a]: R = resolved; M = marginally resolved.
[b]: Transformation of magnitudes to H band done assuming V-H = 3.0, R-H = 2.5 and H-K = 0.2 galaxy colours.
All magnitudes have been converted to our adopted cosmology ($H_0 = 50$ km s^{-1} Mpc^{-1} and $q_0 = 0$).
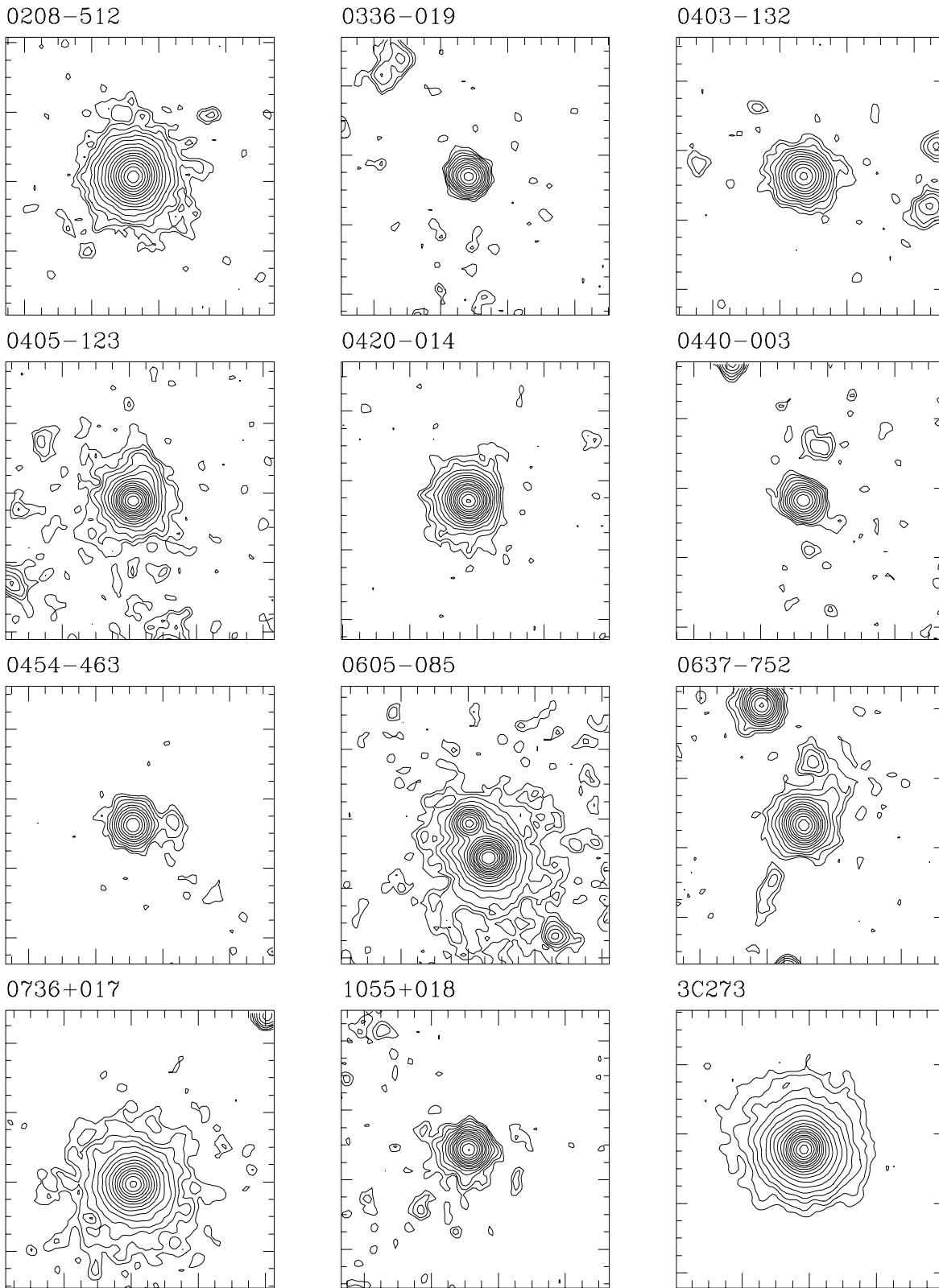
Fig. 1. a Gaussian (σ = 1 px; 0.27$''$) smoothed contour plots of the sample objects in the H band. The full size of the image is 80 px (21.6$''$) across. The contours are separated by 0.5 mag intervals. North is up and east to the left.
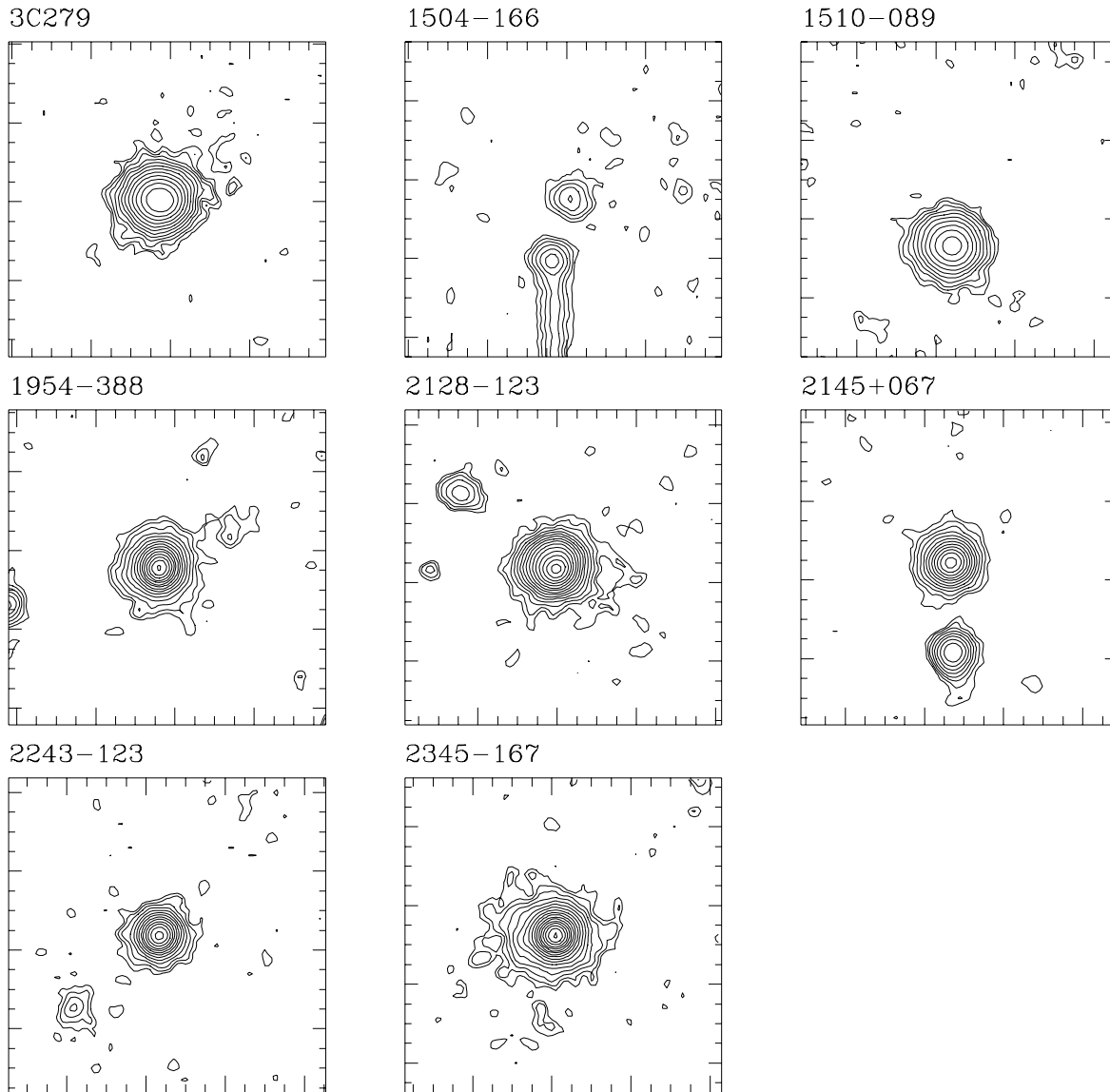
Fig. 1a. (continued)

Considering all these samples together gives average host magnitude of M(H) = -25.9±0.4. As can be seen from Fig. 3, there is no significant difference between the average values of these samples. Considering first conservatively both the resolved and marginally resolved FSRQ hosts gives average host magnitude of M(H) = -26.7±1.2, i.e. slightly brighter but <1σ away from the average RLQ value. On the other hand, considering only the firmly detected FSRQ hosts with z>0.2, the average M(H) = -27.8±0.3, more significantly brighter but still consistent with the low-z RLQs within 3σ. The simplest unified model states that all RLQs are similar; it is therefore not surprising that RLQ and FSRQ hosts are reasonably similar, especially considering the small number of sources analyzed. However, the persistent 1-2 magnitude difference of FSRQ hosts with AGN hosts at lower redshift suggests evolution in the host brightness with

redshift, and/or a relationship of the host luminosity with the nuclear luminosity (see Sect. 4.2).

Lehnert et al. (1992) reported spatially resolved structures in the K band around six RLQ at z~2.3 that, if interpreted as host galaxies, would correspond to extremely luminous galaxies (average host M(H) = -28.8±1.1), ~1-2 mag brighter than the FSRQs at z~0.65. However, within the scatter involved in these numbers, our results appear to be consistent with those of Lehnert et al. (1992), both for the evolutionary trend in the Hubble diagram (see above) and for the trend between the nuclear and host galaxy luminosities (see Sect. 4.2.), and is supporting evidence for the existence of a real upturn in the host luminosity occurring between z~0.5 and z~2, leading from L≥L* hosts at low redshift to the host galaxies of high redshift quasars that are several magnitudes brighter than L* (see Fig. 3). While this type of change is consistent with evolution of the stellar pop-
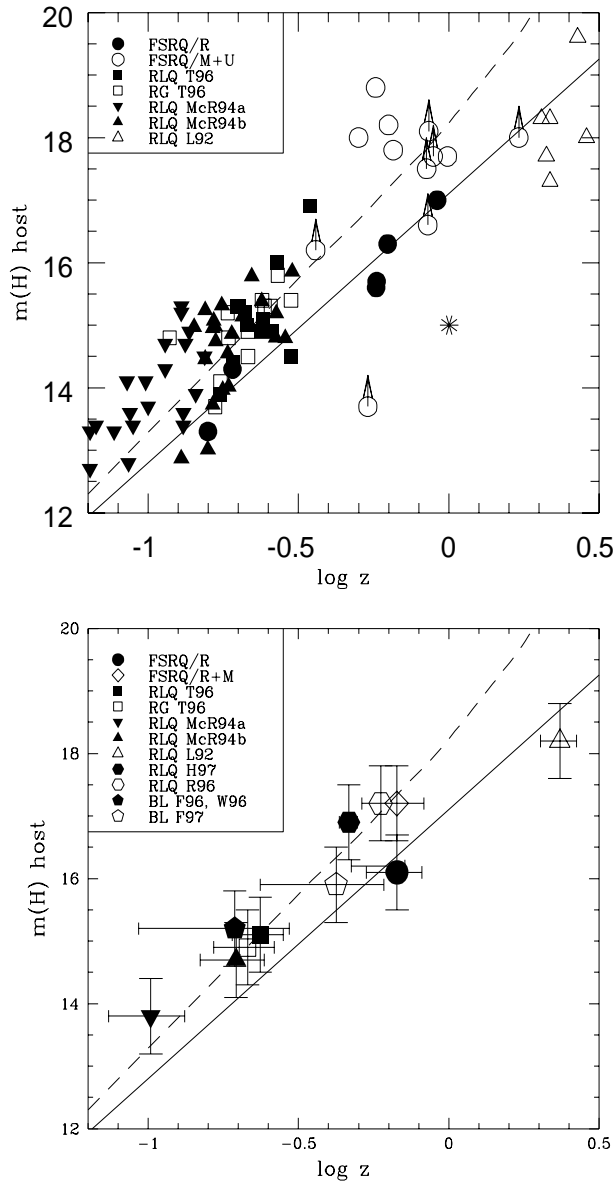
Fig. 2. *Upper panel:* The apparent magnitude of the host galaxies vs. redshift (Hubble diagram). Resolved FSRQs are marked as filled circles, marginally resolved FSRQs as open circles and derived limits for the hosts of unresolved FSRQs as open circles with arrow. PKS 0208-512 is marked as an asterisk (see Appendix at http://link.springer.de). Sources from T96 are marked as filled (RLQ) and open (RG) squares, RLQs from McLeod & Rieke (1994a,b) as solid and inverted solid triangles, and z∼2 RLQs from Lehnert et al. (1992) as open triangles. The solid line is the Hubble relation for RGs (Lilly et al. 1985; Eales et al. 1997). The dashed line is the evolutionary model for elliptical galaxies (Bressan et al. 1994), normalized to the average redshift and magnitude of the low redshift RGs of T96. *Lower panel:* As in the upper panel, except for the mean values of the FSRQs in comparison with samples from literature. The diamond represents the combined sample of resolved and marginally resolved FSRQs, excluding the two low redshift objects (PKS 0736+017 and 3C 273). Additional samples from optical imaging by Rönnback et al. (1996, RLQ), Hooper et al. (1997, RLQ), Falomo (1996, BL Lacs), Wurtz et al. (1996, BL Lacs) and Falomo et al. (1997, BL Lacs) are indicated as marked in the figure.
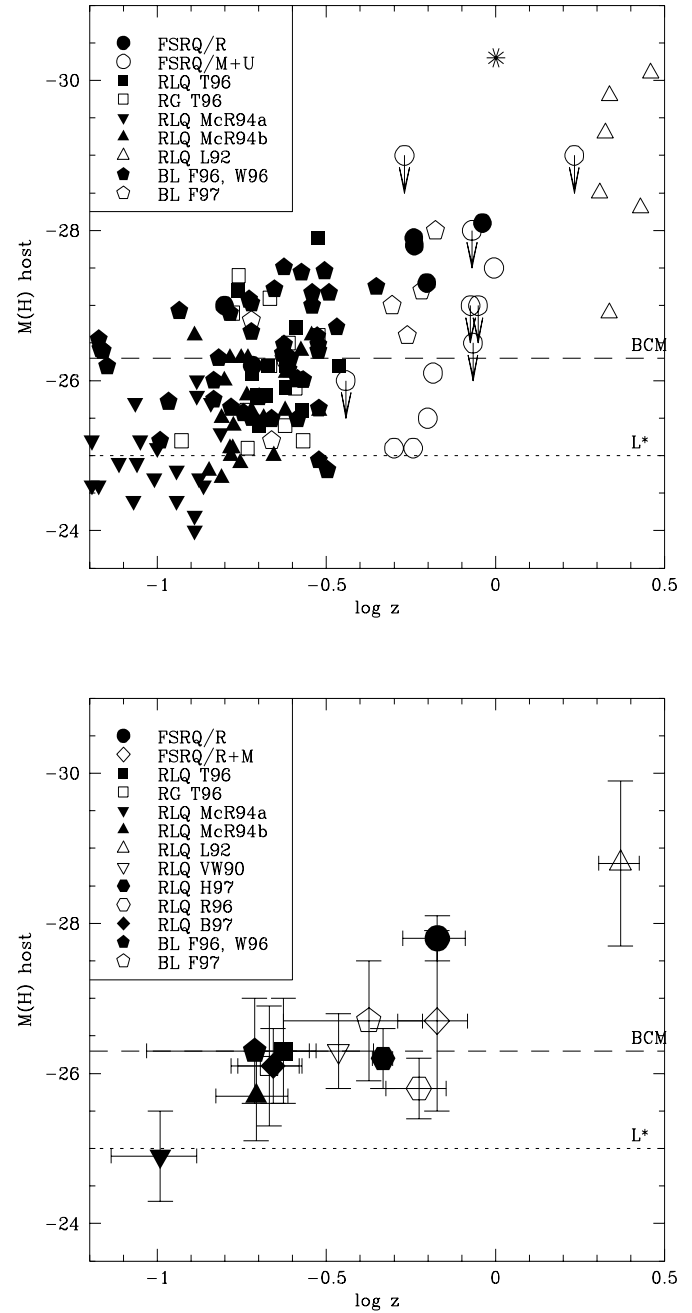
Fig. 3. *Upper panel:* Plot of the absolute H band magnitude of the host galaxies vs. redshift. The average luminosities of L* galaxies (M(H)∼-25.0; Mobasher et al. 1993) and brightest cluster member galaxies (BCM; M(H)∼-26.3; Thuan & Puschell 1989) are indicated as long-dash and short-dash lines,respectively. For symbols, see Fig. 2. *Lower panel:* As the upper panel, except for the mean values of various samples. Additional samples based on optical imaging from Veron-Cetty & Woltjer (1990, RLQ) and Bahcall et al. (1997, RLQ) are indicated as marked in the figure. For other symbols, see Fig. 2.

ulation in the elliptical hosts (as argued for high redshift RGs by Lilly & Longair 1984), or being intrinsic AGN luminosity effect (as argued for high redshift RGs by Eales et al. 1997), there are many caveats in this comparison, most notably differences in the intrinsic quasar luminosity of the various samples. In addition, optical and NIR imaging by Lowenthal et al. (1995) failed to detect extended emission in a sample of six radio-quiet quasars (RQQ) at z∼2.3. Their upper limits indicate that the RQQ hosts at high redshift must be ≤3 mag brighter than L* and ≥1 mag fainter than the Lehnert (1992) sample of RLQs at similar redshift, suggesting that RLQs and RQQs are different types of objects.

While other explanations for light around high redshift RLQs have been proposed, e.g. foreground galaxies producing intervening MgII 2800 Å absorption lines (LeFevre & Hammer 1988) or light from a hidden quasar scattered by dust or electrons along the radio axis (Fabian 1989), starlight from a host galaxy remains the most likely alternative, given that high redshift RGs can reach similar luminosities and the quasar nebulosities follow remarkably well the tight Hubble diagram for RGs (e.g. Lilly 1989; Eales et al. 1997).

There has been considerable disagreement on the similarity between the hosts of RGs and RLQs. While some authors have found similar size and morphology (e.g. Barthel 1989; Veron-Cetty & Woltjer 1990; Lehnert et al. 1992), others have concluded that RLQ hosts are brighter by 0.5-1.0 mag than RGs of similar extended radio emission (e.g. Smith et al. 1986; Hutchings 1987; Smith & Heckman 1989). Abraham, Crawford & McHardy (1992) showed that this disagreement is most likely due to underestimation of RLQ host luminosity due to difficulties in PSF subtraction (because of cosmological host surface brightness dimming and scattered light from the nuclear component), and that RLQ hosts are in fact brighter than RGs. However, using carefully matched samples, T96 found that RLQ and RG hosts are almost identical in morphology, scale length and luminosity, and moreover, the nuclear components of RGs are fainter and redder than those in RLQS, all in good agreement with the unified model. At average redshift z = 0.214±0.049, the average host magnitude of the host galaxies of RGs in the study of T96 is M(H) = -26.1±0.8. This value agrees reasonably well with the higher redshift FSRQ hosts, taking into account some stellar evolution in the early type host galaxies. The data presented in this paper therefore support the similarity between RLQ and RG hosts, considering also the good agreement between the magnitudes of the FSRQ host galaxies and the high redshift RGs used to produce the Hubble diagram (Fig. 2; see Eales et al. 1997).

FSRQs share many properties (e.g. variability and polarization) with BL Lac objects and it is therefore interesting to compare the host properties of these two classes of blazars. Recent optical R band investigations of BL Lac hosts at z≤0.5 by Falomo (1996) and Wurtz et al. (1996) find the average absolute magnitude of the host galaxies to be M(H)∼-25.8 (see Table 4), with some indication of positive correlation of host brightness with increasing redshift. HST R band imaging of a small number of BL Lacs at z>0.5 (Falomo et al. 1997) has provided
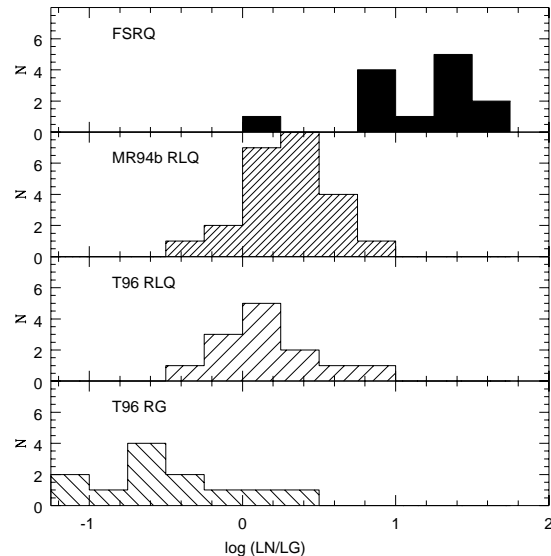
Fig. 4. Histogram of the nucleus/host luminosity ratio for the FSRQs, and for the low redshift RLQs from McLeod & Rieke (1994b) and low redshift RLQs and RGs from T96. The K-band data from T96 has been converted into the H-band assuming colour for the nuclear and galaxy components of H-K = 1.1 and 0.2, respectively.

additional evidence for more luminous hosts (M(H)≤-26.8) at higher redshift. Although based on a small number of resolved objects, it appears therefore that, accounting for stellar evolution that makes galaxies brighter by ∼1 mag between z = 0 and z = 1, the hosts of FSRQs have similar luminosity to lower redshift BL Lacs, in agreement with the unified model. Note also that recent spectroscopic study of the emission line properties (Scarpa & Falomo 1997), which is one of the main distinctive characteristics between FSRQs and BL Lacs, yields additional support to this scenario.

4.2. The nuclear component

The average absolute magnitude of the fitted nuclear component for all FSRQs is M(H) = -29.7±0.8. This indicates that FSRQ nuclei are on average ∼2.5-3 mag brighter than the RLQ nuclei at lower redshift (e.g. T96; M(H) = -27.1±0.8) and ∼4.5-5 mag brighter than the nuclear components in low redshift RGs (e.g. T96; M(H) = -25.1±0.7). The presence of a strong nuclear component in FSRQ is even more evident when considering the nucleus/galaxy (N/G) luminosity ratio, shown in Fig. 4. None of the low redshift RLQs and RGs studied by McLeod & Rieke (1994b) and T96 have N/G >10 in the H band, whereas about half of our FSRQs are above this limit.

From Figs. 2 and 3 it appears that the host galaxies of the various control samples considered here are not dramatically different in intrinsic luminosity, especially if some stellar evolution in the elliptical host galaxies is taken into account. Therefore, Fig. 4 clearly indicates that FSRQs exhibit a nuclear component which is systematically brighter than that of other AGN. This is consistent with the beaming model with large Doppler

amplification factor that makes the observed difference of $\sim$3 magnitudes understandable.

In Fig. 5, we show the relation between the luminosities of the nucleus and the host galaxy for the FSRQs, and for various samples from literature, for individual quasars (upper panel) and for the mean values of the samples (lower panel). While T96 found no convincing correlation between the host and AGN luminosity, we find there is a tendency for the more powerful FSRQs to reside in more luminous hosts. Similar trend has previously been noted in the NIR for low redshift quasars (McLeod & Rieke 1994a,b) and for Seyfert galaxies (Danese et al. 1992; Kotilainen & Ward 1994). Moreover, recent optical observations of bright (M(R)<-24) quasars at 0.4<z<0.5 (Hooper et al. 1997) also indicate what the authors call a positive correlation between the host and nuclear luminosity.

Note that not only the fully and marginally resolved FSRQ hosts, but also all the upper limits derived for the unresolved hosts are well consistent with the boundary limit proposed by McLeod & Rieke (1995) for AGN with M(B)<-23 (solid line in Fig. 5). They interpret the limit in the sense that there is a minimum host galaxy luminosity which increases linearly with quasar luminosity. Recently, McLeod (1997) has speculated that this relationship represents a constant ratio of the central black hole mass to the host galaxy mass. Finally, we advise caution about possible selection effects in this relationship. Since faint host galaxies are difficult to be detected under the most luminous nuclei, we may expect that this contributes to the void of sources in the lower right-hand corner in Fig. 5. On the other hand, in the case of beamed objects such as FSRQs the effects of amplification of the nuclear source may move systematically the points towards larger nuclear luminosities.

5. Summary and conclusions

The main finding of our NIR study is that we can resolve the host galaxies of a significant fraction of luminous AGN out to considerable redshift. The host galaxies of z$\sim$0.65 FSRQs are large (average bulge scale length $\sim$13$\pm$7 kpc) and bright (average M(H)$\sim$-27$\pm$1), much more luminous than L* galaxies (by $\sim$2 mag) and somewhat more luminous than the brightest cluster galaxies (by $\sim$1 mag). Note that all detected hosts have M(H)<-25 ($\sim$L*) and the derived upper limits are consistent with this value. The FSRQ hosts are 1-2 mag brighter than the hosts of lower redshift RLQs, and $\sim$1 mag fainter than the hosts of z$\sim$2 RLQs, consistent with stellar evolution in the elliptical host galaxies and unified models. Finally, the FSRQ hosts appear $\sim$1 mag brighter than the hosts of lower redshift BL Lac objects, again consistent with them forming a common class of blazars, if mild stellar evolution in their host galaxies is assumed.

The luminosity of the host shows a positive trend with that of the active nucleus, at least for the most luminous sources. This enforces the suggestion that, for the brightest AGN, there is a minimum host galaxy luminosity which increases linearly with quasar luminosity. However, since several objects remain unresolved, deeper and higher resolution NIR imaging is required for these sources in order to determine their host properties.
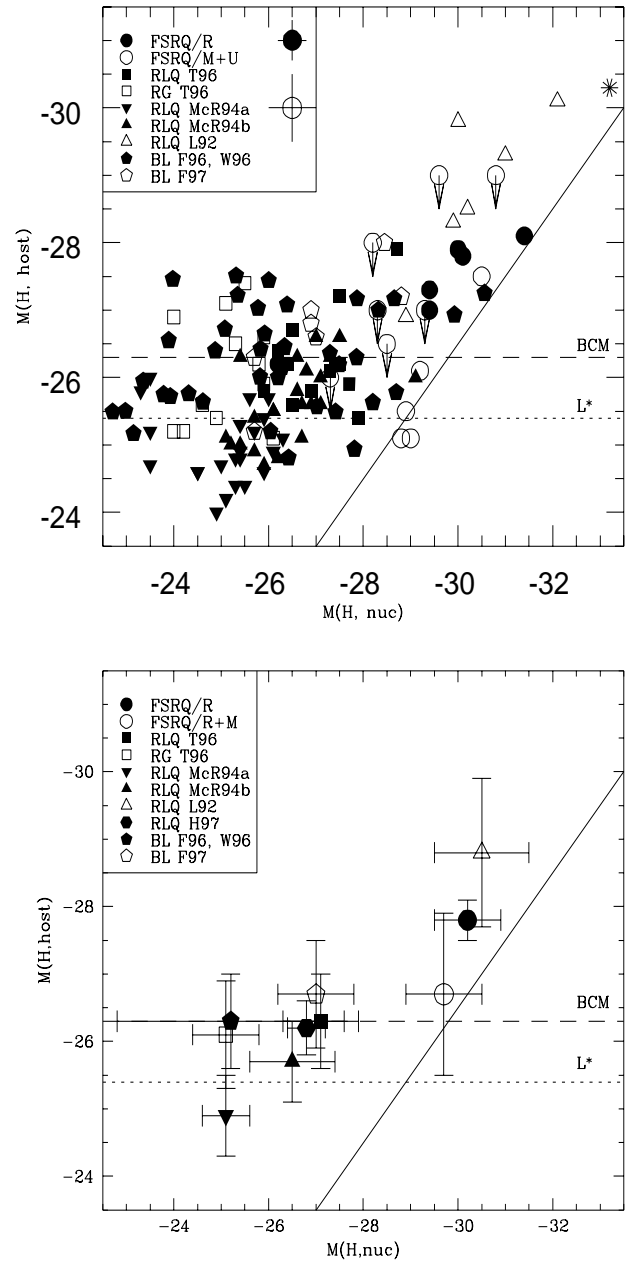
Fig. 5. *Upper panel:* Plot of the H band nuclear vs. host luminosity. For symbols, see Fig. 2 and 3. The solid line is the limiting mass-luminosity envelope from the M(B,nuc) vs. M(H,host) diagram of McLeod & Rieke (1995), converted to H band using a least squares fit of the M(B,nuc) and M(H,nuc) values for the FSRQs from Tables 1 and 3. The two large circles represent the estimated error in the derived host galaxy magnitudes ($\sim$$\pm$0.3 mag for the clearly detected hosts; filled circle, and $\geq$$\pm$0.5 for the marginally detected hosts; open circle). *Lower panel:* As in the upper panel, except for the mean values of various samples. For symbols, see Fig. 2 and 3.

References

Abraham,R.G., Crawford,C.S., McHardy,I.M., 1992, ApJ 401, 474

Antonucci,R.R.J., 1993, ARA&A 31, 473

Bahcall,J.N., Kirhakos,S., Saxe,D.H., Schneider,D.P., 1997, ApJ 479, 642

Barthel,P.D., 1989, ApJ 336, 606

Bersanelli,M., Bouchet,P., Falomo,R., Tanzi,E.G., 1992, AJ 104, 28

Blandford.R.D., Rees,M.J., 1978, Pittsburgh Conference on BL Lac Objects (ed. A.M.Wolfe), 328

Bressan,A., Chiosi,C., Fagotto,F., 1994, ApJS 94, 63

Brindle,C., Hough,J.H., Bailey,J.A., Axon,D.J., Hyland,A.R., 1986, MNRAS 221, 739

Browne,I.W.A., 1983, MNRAS 204, 23P

Capaccioli,M., Caon,N., D'Onofrio,M., 1992, MNRAS 259, 323

Danese,L., Zitelli,V., Granato,G.L. et al. , 1992, ApJ 399, 38

Disney,M.J., Boyce,P.J., Blades,J.C. et al. , 1995, Nat 376, 150

Eales,S., Rawlings,S., Law-Green,D., Cotter,G., Lacy,M., 1997, MNRAS 291, 593

Elvis,M., Wilkes,B.J., McDowell,J.C. et al. , 1994, ApJS 95, 1

Fabian,A.C., 1989, MNRAS 238, 41P

Falomo,R., 1996, MNRAS 283, 241

Falomo,R. et al. , 1997, Proc. ESO-IAC Conference on Quasar Hosts, in press

Fugmann,W., 1988, A&A 205, 86

Gear,W.K., Brown,L.M.J., Robson,E.I. et al. , 1986, ApJ 304, 295

Glass,I.S., 1981, MNRAS 194, 795

Hooper,E.J., Impey,C.D., Foltz,C.B., 1997, ApJ 480, L95

Hutchings,J.B., 1987, ApJ 320, 122

Hutchings,J.B., Neff,S.G., 1991, PASP 103, 26

Hutchings,J.B., Neff,S.G., 1992, AJ 104, 1

Hyland,A.R., Allen,D.A., 1982, MNRAS 199, 943

Impey,C.D., Tapia,S., 1990, ApJ 354, 124

Kidger,M.R., Garcia-Lario,P., de Diego,J.A., 1992, A&AS 93, 391

Kotilainen,J.K., Ward,M.J., 1994, MNRAS 266, 953

Landolt,A., 1992, AJ 104, 340

LeFevre,O., Hammer,F., 1988, ApJ 333, L37

Lehnert,M.D., Heckman,T.M., Chambers,K.C., Miley,G.K., 1992, ApJ 393, 68

Lepine, J.R.D., Braz,M.A., Epchtein,N., 1985, A&A 149, 351

Lilly,S.J., 1989, ApJ 340, 77

Lilly,S.J., Longair,M.S., 1984, MNRAS 211, 833

Lilly,S.J., Longair,M.S., Allington-Smith,J.R., 1985, MNRAS 215, 37

Litchfield,S.J., Robson,E.I., Stevens,J.A., 1994, MNRAS 270, 341

Lowenthal,J.D., Heckman,T.M., Lehnert,M.D., Elais,J.H., 1995, ApJ 439, 588

McAlary,C.W., McLaren,R.A., McGonegal,R.J., Maza,J., 1983, ApJS 52, 341

McLeod,K.K., 1997, Proc. ESO-IAC Conference on Quasar Hosts, in press

McLeod,K.K., Rieke,G.H., 1994a, ApJ 420, 58

McLeod,K.K., Rieke,G.H., 1994b, ApJ 431, 137

McLeod,K.K., Rieke,G.H., 1995, ApJ 454, L77

Mead,A.R.G., Ballard,K.R., Brand,P.W.J.L. et al. , 1990, A&AS 83, 183

Mobasher,B., Sharples,R.M., Ellis,R.S., 1993, MNRAS 263, 560

Moffat,A.F.J., 1969, A&A 3, 455

Moorwood,A.F.M. et al. , 1992, ESO Messenger 69, 61

Neugebauer,G., Oke,J.B., Becklin,E.E., Matthews,K., 1979, ApJ 230, 79

Neugebauer,G., Matthews,K., Soifer,B.T., Elais, J.H., 1985, ApJ 298, 275

O'Dell,S.L., Puschell,J.J., Stein,W.A., Warner,J.W., 1978, ApJS 38, 267

Padovani,P., 1992, MNRAS 257, 404

Padovani,P., Urry,C.M., 1992, ApJ 387, 449

Quirrenbach,A. Witzel,A., Krichbaum,T.P. et al. , 1992, A&A 258, 279

Roellig,T.L., Becklin,E.E., Impey,C.D., Werner,M.W., 1986, ApJ 304, 646

Rönnback,J., van Groningen,E., Wanders,I., Örndahl,E., 1996, MNRAS 283, 282

Sambruna, R.M., 1997, ApJ 487, 536

Scarpa,R., Falomo,R., 1997, A&A 325, 109

Sitko,M.L., Sitko,A.K., 1991, PASP 103, 160

Sitko,M.L., Stein,W.A., Zhang,Y.X., Wisniewski,W.Z., 1983, PASP 95, 742

Smith,E.P., Heckman,T.M., Bothun,G.D., Romanishin,W.R., Balick,B., 1986, ApJ 306, 64

Smith,E.P., Heckman,T.M., 1989, ApJ 341, 658

Stickel,M., Padovani,P., Urry,C.M., Fried,J.W., Kühr,H., 1991, ApJ 374, 431

Sun,W.H., Malkan,M.A., 1989, ApJ 346, 68

Taylor,G.L., Dunlop,J.S., Hughes,D.H., Robson,E.I., 1996, MNRAS 283, 930 (T96)

Thuan,T.X., Puschell,J.J., 1989, ApJ 346, 34

Tyson,J.A., Baum,W.A., Kreidl,T., 1982, ApJ 257, L1

Ulrich,M.H., 1989, BL Lac Objects, p. 45

Urry,C.M., Padovani,P., 1995, PASP 107, 803

Vermeulen,R.C., Cohen,M.H., 1994, ApJ 430, 467

Veron-Cetty,M-.P., Woltjer,L., 1990, A&A 236, 69

von Montigny,C. et al. , 1995, ApJ 440, 525

Wall,J.V., Peacock,J.A., 1985, MNRAS 216, 173

Wills,B., 1976, AJ 81, 1507

Wright,A.E., Ables,J.G., Allen,D.A., 1983, MNRAS 205, 793

Wurtz,R., Stocke,J.T., Yee,H.K.C., 1996, ApJS 103, 109

Wyckoff,S., Wehinger,P.A., Gehren,T. et al. , 1980, ApJ 242, L59